STATISTICAL ANALYSIS OF SCATTEROMETER MEASUREMENT CORRELATION

Peter Yoho
Brigham Young University, 484 CB, Provo, UT 80601
(801) 422-4884 yoho@byu.edu

***Abstract*— Satellite scatterometers have gained in popularity recently due to expanded application of their data. New instruments are being developed which oversample the surface to improve the resolution of data, furthering application development. Such oversampling introduces the possibility of correlation between measurements, an issue which has previously been irrelevant due to the lower sampling rates of past instruments. This paper derives a mathematical expression for correlation between consecutive scatterometer measurements. Since measurement correlation is dependent upon instrument configuration, a general methodology is presented so that the algorithm can be adapted to specific instruments. An analysis of the expressions is provided. An adaptation of correlation effects on NASA's most recent scatterometer, SeaWinds, is provided.**

I. Introduction

SATELLITE scatterometers have generated increased interest in the last few years by demonstrating an ability to not only estimate ocean wind speed and direction, their original motivation, but to also investigate iceberg location, snow melt cycles, and tropical deforestation. Emergence of these new application has sparked the development of new instruments and new algorithms, both seeking to improve the data quality and resolution of the measurements.

In particular, instruments are using larger antennas and higher pulse rates to obtain a more dense sampling of the surface of interest. The significant increase in sampling density has introduced an issue which has not previously been explored - that of correlation between measurements. This paper addresses the issue of correlation between measurements, caused by oversampling of the surface. Correlation not only decreases the amount of new information obtained by a measurement, but also increases the variance of the measurement, degrading its accuracy and quality.

This paper presents the mathematical theory related to measurement correlation. Since actual values are instrument specific, we present a general methodology for determining their values. The paper is organized as follows. Section II presents theory relevant to the discussion of multiple, overlapping measurements by describing the statistics of signal scattering. Section III then presents a measurement framework relating to general scatterometer measurements. The section analyzes the correlation and covariance expressions and their dependence on basic scattering principles and the general measurement methodology. Section IV provides an analysis of the covariance expression and how measurement design can be optimized to limit measurement correlation. It then applies the theory to NASA's most recent scatterometer, SeaWinds on QuikSCAT. Finally, Section V summarizes findings and concludes.

II. Surface Scattering of Distributed Targets

When a microwave signal impacts a conductive surface a portion of the signal energy is reflected back towards the origin of the incident wave. This reflection is termed backscatter. The voltage backscattered by a single object can be represented by the complex value z_i, where $z_i = r_i + jq_i$. For spaceborne instruments, when the transmitted signal intersects the earth's surface it is simultaneously incident on a large number of scatterers. The backscatter response from a large number of point targets, termed a distributed target, is the sum of the response from the individual point scatterers,

$$Z_d = \sum_i z_i = V_d e^{j\phi_d}. \tag{1}$$

Applying the central limit theorem (by assuming that there are a large number of scatterers in the distributed response) and assuming that no single scatterer dominates the overall return, the real and imaginary parts of the individual responses, r_i and q_i, may be assumed to be independent, normally distributed random variables. In this case, the magnitude of the distributed target, V_d, has a Rayleigh distribution, and the phase response, ϕ_d, is uniformly random over the interval ($[0, 2\pi]$) [1].

The expected value of the voltage magnitude, V_d, is

$$\mathcal{E}[V_d] = \sqrt{\frac{\pi}{2}}\sigma, \tag{2}$$

where $\mathcal{E}$ is the expected value operator and σ is the standard deviation of r_i and q_i. The second moment of the voltage magnitude is

$$\mathcal{E}[V_d^2] = 2\sigma^2. \tag{3}$$

We assume that V_d and ϕ_d are independent for each small area or resolution element considered. This is reasonable considering that most surface features have sub-meter correlation lengths and most scatterometer measurements encompass several square kilometers.

We now define the backscattered power of the distributed target, P_d, as the square of the backscattered voltage,

$$P_d = V_d^2 \tag{4}$$

so that

$$\mathcal{E}[P_d] = \mathcal{E}[V_d^2] = 2\sigma^2 = A_d\sigma_d^\circ \tag{5}$$

where A_d is the area of the distributed target and σ° is the normalized radar cross section of the area, which is proportional to the variance of the individual scatterers.

The correlation between two separate distributed targets, a and b, can then be written as

$$\begin{aligned}\mathcal{E}[Z_d(a)Z_d^*(b)] &= \mathcal{E}[V_d(a)V_d(b)]\mathcal{E}[e^{j[\phi_d(a)-\phi_d(b)]}] &(6)\\ &= \mathcal{E}[V_d(a)V_d(b)]\delta(a-b) &(7)\\ &= \mathcal{E}[V_d^2(a)]\delta(a-b) &(8)\\ &= A_d\sigma_d^\circ\delta(a-b). &(9)\end{aligned}$$

III. Instrument Measurement

A scatterometer transmits a known signal,

$$\xi_t(t) = \sqrt{E_t}a(t)e^{j\omega_c t} \tag{10}$$

where t is time, E_t is the total transmitted energy for a single pulse, ω_c is the angular center frequency, and $a(t)$ is the complex modulation function given by

$$\int_0^{T_p} |a(t)|^2 \, \mathrm{d}t = 1 \tag{11}$$

with $a(t) = 0$ for $t < 0$, $a(t) > 0$ for $0 \le t \le T_p$, and $a(t) = 0$ for $t > T_p$.

Ignoring the spreading loss and antenna gain for the moment, the echo of the signal from a single point scatterer can be written as

$$\xi_p(t) = z_i\left(\sqrt{E_t}a(t-2r/c)e^{j\omega_c t}e^{-j\omega_d(x,y)t}e^{j2\omega_c r/c}\right), \tag{12}$$

where r is the range from instrument to the point scatterer, and ω_d is the Doppler shift of the point. This assumes that changes in the spacecraft velocity need not be considered in the Doppler shift, which generally holds when pulse periods are less than 1 second and center frequencies are greater than 1 GHz [2]. Accounting for antenna gain and spreading loss terms, the return signal echo for the i^{th} scatterer can be written as

$$\xi_r(t,i) = z_i\left(\frac{G(i)\lambda}{(4\pi)^{3/2}r^2(i)}\right)\cdot \left(\sqrt{E_t}a(t-2r(i)/c)e^{j\omega_c t}e^{-j\omega_d(i)t}e^{j2\omega_c r(i)/c}\right), \tag{13}$$

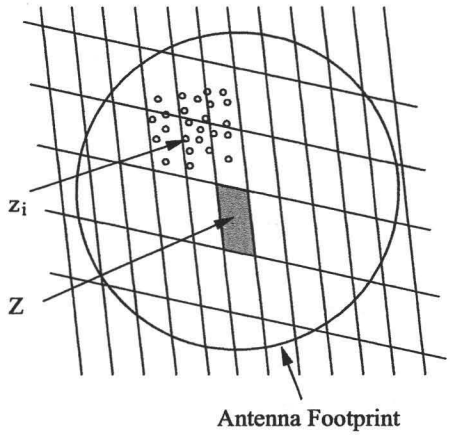

Fig. 1. Basic geometry of a scatterometer footprint. Each z_i represents an individual scatterer, while Z represents the total voltage response of one resolution element, consisting of multiple individual scatterers. The footprint is the 3 dB contour of the illumination pattern.

where λ is the signal's wavelength, and G is the antenna gain in the direction of the point scatterer.

While we might desire to measure the response of each individual scatterer, limitations of Doppler and range filtering constrain the resolution of actual measurements. Without some form of Doppler or range filtering, the resolution of a measurement is limited to the size of the antenna footprint, typically described using its 3 dB beam width. Utilizing Doppler and/or range filtering can improve the effective resolution of the instrument by separating the antenna footprint into multiple resolution elements. Figure 1 illustrates the footprint geometry for a scatterometer measurement. The large, bold circle represents a generic antenna footprint and the lines represent an arbitrary resolution grid generated by range and Doppler filtering. For spaceborne scatterometers, antenna footprint widths are on the order of tens of kilometers or more and filtered resolution elements are typically several square kilometers. In both cases, the large size allows us to assume, as previously mentioned, that a large number of scatterers, z_i, exist in each resolution element, Z, which is considered to be one distributed target ($Z_d \equiv Z$).

Recognizing these resolution limitations, the measured return signal (13) can be defined as the sum of the individual point scatterers within each resolution element,

$$\xi_r(t,n) = \frac{\sqrt{E_t}\lambda}{(4\pi)^{3/2}}\sum_{i_n} z_{i_n}\cdot \frac{G(i_n)a(t-2r(i_n)/c)e^{j\omega_c t}e^{-j\omega_d(i_n)t}e^{j2\omega_c r(i_n)/c}}{r^2(i_n)}, \tag{14}$$

where the sum is over the i scatterers in the n^{th} resolution element. For a satellite, the range term is very large in comparison to the change in range for each resolution element, we therefore assume that the denominator, r^2, is constant over the sum for each resolution element and use the mean value for the measurement, $\bar{r}^2$. For simplicity, we also assume that gain and observed Doppler are constant over each resolution element. Using a standard (x, y) coordinate system, aligned with the along track and cross track directions, along with (1), the return signal can now be defined by

$$\xi_r(t,x,y) = \frac{\sqrt{E_t}\lambda}{(4\pi)^{3/2}\bar{r}^2} Z(x,y)G(x,y)\cdot a(t-2r(x,y)/c)e^{j\omega_c t}e^{-j\omega_d(x,y)t}e^{j2\omega_c r(x,y)/c}. \tag{15}$$

Equation (15) defines the generalized return signal for a scatterometer. The process which scatterometer instruments use to measure this signal varies from instrument to instrument, depending upon requirements for resolution, the instrument modulation function, $a(t)$, and the receiver hardware available. In general, instruments use a form of square-law detection which can be written as

$$M^s = \Omega\left|\Omega\xi_r(t,x,y)\right|^2 \tag{16}$$

where the Ω operator is an element of the set

$$\Omega \in \left\{\int, \iint, \sum, \sum\sum\right\} \tag{17}$$

and sums (either discretely or continuously) over the x-y area and time as required by the specific instrument.

For this paper, we will define the measurement of the return signal, M^s, as

$$M^s = \int_{T_a}^{T_b}\left|\int_{x_a}^{x_b}\int_{y_a}^{y_b}\xi_r(t,x,y)\,\mathrm{d}y\,\mathrm{d}x\right|^2 \mathrm{d}t, \tag{18}$$

where T_a and T_b span the time limits of pulse integration, x_a and x_b delimit the footprint in the range direction, and y_a and y_b delimit the footprint in the Doppler direction. We choose this form for its correspondence with several past scatterometers. We recognize that for many instruments the limits of integration for range and Doppler will be interdependent; for simplicity we define these limits as independent. For later use, let us also define the inner portion of (18) as

$$\zeta(t) = \int_{x_a}^{x_b}\int_{y_a}^{y_b}\xi_r(t,x,y)\,\mathrm{d}y\,\mathrm{d}x \tag{19}$$

so that

$$M^s = \int_{T_a}^{T_b}|\zeta(t)|^2\,\mathrm{d}t. \tag{20}$$

We also define the radar calibration parameter, X, as

$$X = \frac{E_t\lambda^2 G_o^2 A_E}{(4\pi)^3\bar{r}^4}, \tag{21}$$

with G_o the peak antenna gain, and A_E the effective measurement area,

$$A_E = \frac{1}{G_o^2}\int_{x_a}^{x_b}\int_{y_a}^{y_b}G^2(x,y)A_d(x,y)\,\mathrm{d}y\,\mathrm{d}x. \tag{22}$$

We can then use (9) and the fact that G is purely real to show that the expected value of the measurement is

$$\mathcal{E}[M^s] = \frac{X}{G_o^2 A_E}\int_{T_a}^{T_b}\int_{x_a}^{x_b}\int_{y_a}^{y_b}A_d(x,y)\sigma^\circ(x,y)\cdot G^2(x,y)|a(t-2r(x,y)/c)|^2\,\mathrm{d}y\,\mathrm{d}x\,\mathrm{d}t. \tag{23}$$

We can make a further simplifying assumption, that σ° is constant over the measurement area, to obtain

$$\mathcal{E}[M^s] = X\sigma^\circ H \tag{24}$$

where H is

$$H = \frac{1}{G_o^2 A_E}\int_{T_a}^{T_b}\int_{x_a}^{x_b}\int_{y_a}^{y_b}A_d(x,y)\cdot G^2(x,y)|a(t-2r(x,y)/c)|^2\,\mathrm{d}y\,\mathrm{d}x\,\mathrm{d}t. \tag{25}$$

Using a similar process, we can also find the autocorrelation of the signal from a specific resolution element

$$\mathcal{E}[\zeta(t)\zeta^*(\tau)] = X\sigma^\circ L(t,\tau) \tag{26}$$

by assuming, as before, that σ° is constant over the measurement area, and by defining L as

$$L(t,\tau) = \frac{1}{G_o^2 A_E}\int_{x_a}^{x_b}\int_{y_a}^{y_b}A_d(x,y)G^2(x,y)a(t-2r(x,y)/c)\cdot a^*(\tau-2r(x,y)/c)e^{j\omega_c(t-\tau)}e^{-j\omega_d(x,y)(t-\tau)}\,\mathrm{d}y\,\mathrm{d}x \tag{27}$$

A. Multiple Pulses

The general statistical properties of scatterometer measurements have been calculated for several different instruments [3], [4], [5]. These studies have focused on the properties of single, independent measurements and are well understood. It is our desire to extend the theory to recent designs by considering correlated measurements. Using definitions and methods similar to the above derivation, and again assuming for that $\sigma^\circ(x,y)$ is homogeneous across the integration area, the correlation of two measurements, M_k^s and M_l^s can be written as

$$\mathcal{E}[M_k^s M_l^s] = X_k X_l \sigma_k^\circ \sigma_l^\circ [H_k H_l + W] \tag{28}$$

where W is

$$W = \int_{T_a}^{T_b}\int_{T_a'}^{T_b'}\int_{x_a}^{x_b}\int_{y_a}^{y_b}\int_{x_a'}^{x_b'}\int_{y_a'}^{y_b'} A_{e,1}(x,y)A_{e,2}(x',y')G_k(x,y)\cdot G_k(x',y')G_l(x',y')G_l(x,y)a_k(t-2r(x,y)/c)\cdot a_k^*(t-2r(x',y')/c)a_l(\tau-2r(x',y')/c)\cdot a_l^*(\tau-2r(x,y)/c)e^{-j(\omega_d(x,y)t-\omega_d(x',y')t}\cdot e^{j(\omega_d(x',y')\tau-\omega_d(x,y)\tau)}\,dy'\,dx'\,dy\,dx\,dt\,d\tau. \tag{29}$$

The covariance, $Cov[M_k\, M_l]$, of two measurements can be shown to be

$$Cov[M_k\, M_l] = \sigma_k^\circ \sigma_l^\circ X_k X_l W. \tag{30}$$

Equations (28) and (30) show that the value of the correlation and covariance is directly related to W, which is the only term that is dependent on both measurements, M_k^s and M_l^s. If the measurements are of the same area ($k = l$), the correlation simplifies to the second moment of the measurement,

$$\mathcal{E}[(M^s)^2] = (X\sigma^\circ)^2[H^2 + W], \tag{31}$$

and the covariance equals the variance of the measurement, $(\sigma^\circ X)^2 V$ where V is equivalent to W when reduced to the single measurement form [4]. If, on the other hand, the measurements M_k^s and M_l^s are completely independent, the W term is zero, the covariance is zero, and the correlation is just the square of the expected value, $\mathcal{E}^2[M^s]$.

IV. Analysis of the Covariance Expression

The key term on which both the correlation and covariance expressions, (28) and (30), depend is the W term. Our interest then is to understand the behavior of W when the two measurements have partial overlap, either in the along track or cross-track directions.

In order to gain an understanding of W, we employ a few simplifications to provide clarity. First we will assume that A_d is uniform for all differential elements and thus becomes a constant. Next, we introduce the generalized radar ambiguity function [1]

$$\mathcal{X}(t,f) = \int_{-\infty}^{+\infty} a(y)a^*(y+t)e^{j2\pi fy}\,dy. \tag{32}$$

and use a change of variables substitution, $y = t - 2r(x',y')/c$ in (29). We note that $a(t)$ is zero outside the time limits of the pulse and assume that the range gates are sufficiently wide to admit all of the echo signal. This allows us to extend the time limits of (29) to infinity without effecting the total value of the integral. Implementing these changes, W can be written as

$$W = \int_{x_a}^{x_b}\int_{y_a}^{y_b}\int_{x_a'}^{x_b'}\int_{y_a'}^{y_b'} Q(x,y)Q(x',y')\cdot \mathcal{X}_k(p,k)\mathcal{X}_l^*(p,k)\,dy'\,dx'\,dy\,dx \tag{33}$$

where $p = \frac{2}{c}[r(x',y') - r]$ and $k = \frac{1}{2\pi}[\omega_d(x,y) - \omega_d(x',y')]$, and $Q(x,y) = G_k(x,y)G_l(x,y)$.

The characteristics of the radar ambiguity function are determined by the pulse modulation function, $a(t)$. The ambiguity function for a linear frequency modulated (LFM) pulse ("chirped") is often referred to as a "razor blade" due to its sharp diagonal peak, as shown in Fig-

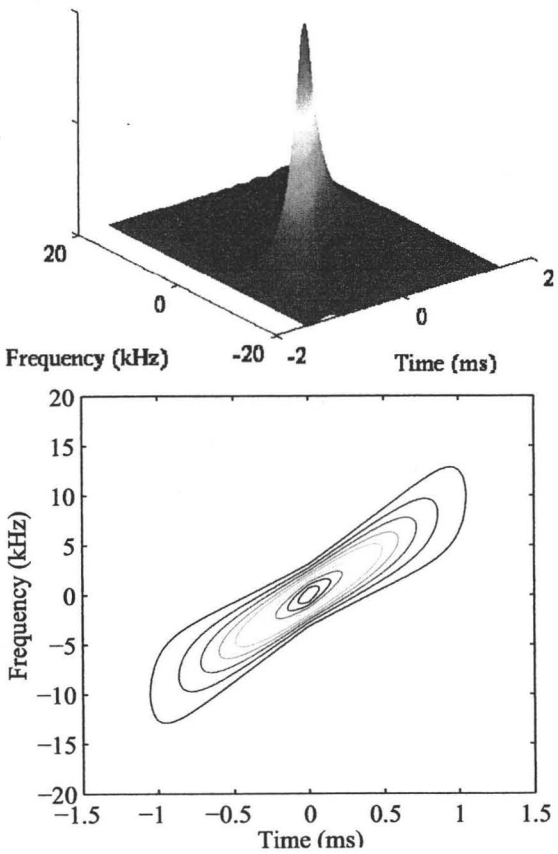

Fig. 2. Radar ambiguity function for a general LFM modulated pulse (32).

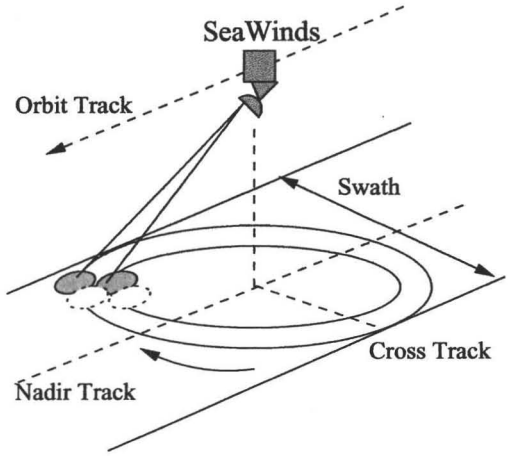

Fig. 3. Measurement geometry for SeaWinds [5].

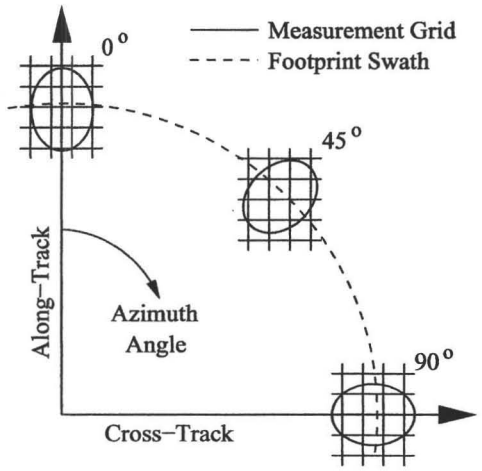

Fig. 4. Along track and cross track grid lines for three cell locations during a rotation [4].

ure 2. The width of the peak in the time dimension is determined by the duration of the pulse and the width of the response in the frequency direction is proportional to the reciprocal of the pulse repetition period. The angle between time and frequency is determined by the chirp rate.

An instructive approach to understanding the expression for W is to calculate it as a function of position offset between the two pulses, in the x and y directions. We define the first pulse to be centered about the origin so that for $\Delta x = x_b - x_a$ and $\Delta y = y_b - y_a$ we have $x_a = -\Delta x/2$, $x_b = \Delta x/2$, $y_a = -\Delta y/2$, and $y_b = \Delta y/2$, and $x'_a = X - \Delta x/2$, $x'_b = X + \Delta x/2$, $y'_a = Y - \Delta y/2$, and $y'_b = Y + \Delta y/2$. The figures in the following section are plotted using this convention. The level curves of the contour plots are placed at 0.1 increments.

A. Application to SeaWinds

Relating the effects of correlation to actual instruments requires understanding the way the instruments make their measurements. For this paper we will consider the recently developed pencil-beam scatterometer SeaWinds. SeaWinds operates by conically scanning about nadir a pencil beam antenna. It operates at an elevation of approximately 800 km, having a ground speed of 7 km/s. It has two beams, an inner and outer, alternating pulses between the beams. For our discussion, we will only consider the outer beam, which has a footprint of 36 km x 26 km, an elevation angle of 45 degrees and a 3 dB beam width of 1.4°. SeaWinds transmits 1.5 ms pulses every 5.4 ms, each having a bandwidth of 375 kHz. It's antenna rotates at a rate is 18 rpm, thus offsetting each pulse by about 1.17° for the same beam. Figure 3 describes the geometry of

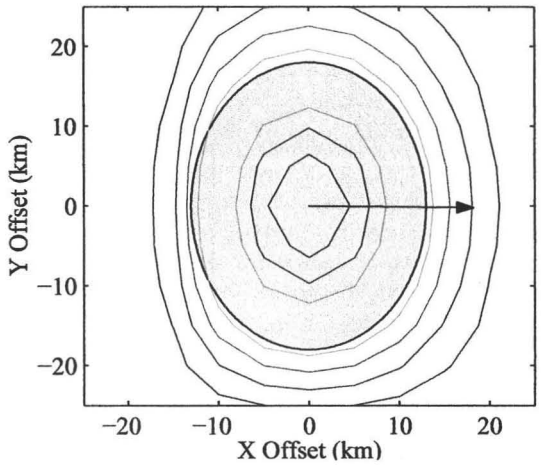

Fig. 5. Correlation contours for SeaWinds at 0° azimuth. The arrow represents the location of the next pulse, (18.25 km, -0.19 km). The normalized correlation coefficient is 0.19.

SeaWinds.

The footprint, or illuminated area of the surface, can be segmented, as described previously, into pieces using several coordinate systems. The most intuitive, a rectangular, (x, y) grid, is defined using the nadir track and cross track axes defined in figure 3. As the antenna rotates about nadir, the illuminated area also moves, changing the orientation of the along and cross track grid. Figure 4 illustrates this change for three cell locations during the rotation. Using Figure 4 the geometry of the footprint can be related to the

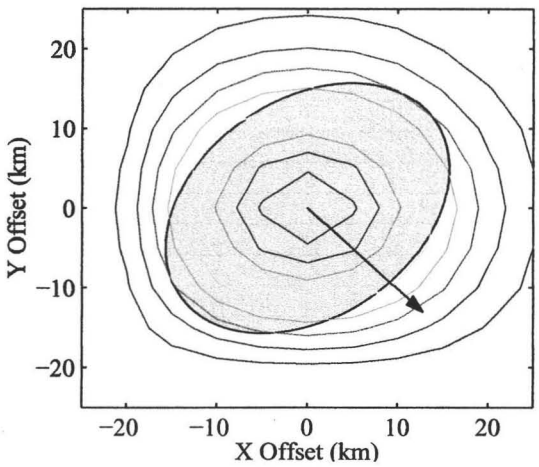

Fig. 6. Correlation contours for SeaWinds at 45° azimuth. The arrow represents the position of the consecutive pulse, (12.78 km, -13.04 km). The normalized correlation coefficient is 0.27.

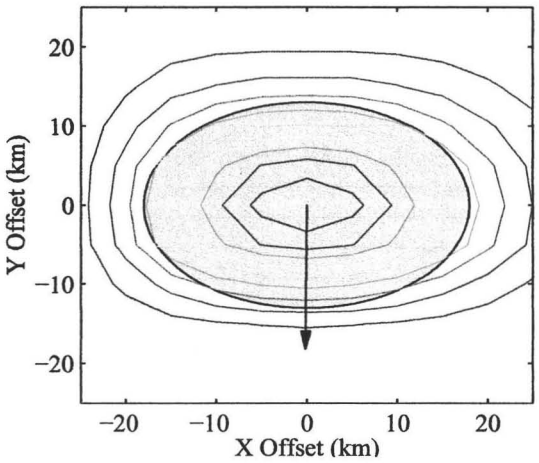

Fig. 7. Correlation contours for SeaWinds at 90° azimuth. The arrow represents the position of the consecutive pulse, (-0.19 km, -18.25 km). The normalized correlation coefficient is 0.02.

geometry of the expression for W and offset parameters (X, Y). For presentation, we describe the correlation for consecutive pulses using the three depicted azimuth angles, 0°, 45°, and 90°, shown in Figures 5, 6, and 7 respectively. Each figure shows the normalized correlation values for combination offsets in both along track and cross track directions. The figures show that the next pulse will be offset by $(18.25km, -0.19km)$ at 0°, $(12.78km, -13.04km)$ at 45°, and $(-0.19km, -18.25km)$ at 90°. Furthermore, they show that the normalized correlation coefficient W has a value of 0.19, 0.27, and 0.02 respectively.

The value of this correlation is significant because it reduces the amount of new information present in the consecutive pulse and also increased the variance of the signal. Signal variance is a factor of the number of independent "looks", N_l, or samples of the surface and is of the form

$$\sigma_N^2 = \frac{\sigma_1^2}{N_l} \tag{34}$$

where σ_N^2 is the variance of the multiple look measurement and σ_1^2 is the variance of the single look measurement. For scatterometers, the number of looks can be approximated by the time bandwidth product of the measurement, $T_r B_r$, where $T_r = T_b - T_a$ and B_r is the bandwidth of the instrument hardware. Multiple measurements provide additional looks, with the total number of looks being $N_p N_l$ for N_p independent pulses. However, if the measurements are correlated, the number of looks is reduced to $[N_p(1-\rho)]\, N_l$, thus degrading the accuracy of the measurements.

V. Summary

Surface oversampling has the possibility of improving measurement resolution by providing significantly more data than previously available. However, the amount of information available is limited by the correlation of the measurements. The correlation coefficient of a given measurement is determined by the size of the antenna footprint and the implementation of pulse modulation function.

One additional consideration not mentioned in the publication is the presence of random additive noise. This noise, which is caused by radiation incident on the instrument antenna, as well as internal thermal variation also degrades the performance of the instrument. Actual instrument designs take this issue into consideration.

A basic analysis of the cross covariance expression was presented for the SeaWinds instrument. More modern instruments, still in the design phase, plan on sampling significantly more dense than SeaWinds. The likelihood of large correlation coefficients is significant and merits additional consideration.

References

[1] F. Ulaby, R. Moore, and A. Fung, *Microwave Remote Sensing: Active and Passive.* Norwood, Massachusetts: Artech House, Inc., 1986, vol. 2.

[2] D. G. Long, "The derivation of a generalized Kp equation for a spaceborne pencil-beam scatterometer," Brigham Young University, Tech. Rep. MERS 95-004, TR-L106-95.4, June 1995.

[3] R. Fisher, "Standard deviation of scatterometer measurements from space," *IEEE Trans. Geosci. Electron.*, vol. GE-10, April 1972.

[4] D. G. Long and M. W. Spencer, "Radar backscatter measurement accuracy for a spaceborne pencil-beam wind scatterometer with transmit modulation," *IEEE Trans. Geosci. Remote Sensing*, vol. 35, no. 1, pp. 102–114, January 1997.

[5] M. W. Spencer, C. Wu, and D. G. Long, "Improved resolution backscatter measurements with the SeaWinds pencil-beam scatterometer," *IEEE Trans. Geosci. Remote Sensing*, vol. 38, no. 1, pp. 89–104, January 2000.